Supplementary Information

Mono- and Bimetallic Amidinate Samarium Complexes - Synthesis, Structure, and Hydroamination Catalysis

Neda Kazeminejad,[a] Luca Münzfeld,[a] Michael T. Gamer,[a] and Peter W. Roesky*[a]

[a] Institute of Inorganic Chemistry Karlsruhe Institute of Technology (KIT), Engesserstraße 15, 76131 Karlsruhe (Germany).

Table of contents

X-ray Crystallographic Studies

Suitable crystals were covered in mineral oil (Aldrich) and mounted on a glass fiber or MiTeGen holder. The crystals were transferred directly to the cold stream of a STOE IPDS 2 diffractometer.

All structures were solved by using the program SHELXS/T[1, 2] and Olex2.[3] The remaining non-hydrogen atoms were located from successive difference Fourier map calculations. The refinements were carried out by using full-matrix least-squares techniques on F^2 by using the program SHELXL.[1, 2] In each case, the locations of the largest peaks in the final difference Fourier map calculations, as well as the magnitude of the residual electron densities, were of no chemical significance.

Crystallographic data (excluding structure factors) for the structures reported in this paper have been deposited with the Cambridge Crystallographic Data Centre as a supplementary publication no. 1904969-1904970. Copies of the data can be obtained free of charge on application to CCDC, 12 Union Road, Cambridge CB21EZ, UK (fax: (+(44)1223-336-033; email: deposit@ccdc.cam.ac.uk).

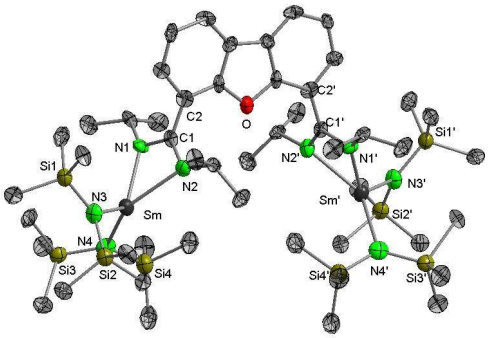

Figure S1. Molecular structure of [Sm(^{Dipp}L$_{Ph}$){N(SiMe$_3$)$_2$}$_2$] (**1**) in the solid state (displacement ellipsoids are scaled to the 30% probability level; omitting carbon bound hydrogen atoms for clarity). Selected bond lengths [Å], angles [°]: Sm-Sm 8.8839(13), Sm-N1 2.37(2), Sm-N2 2.42 (2), Sm-N3 2.282(14), Sm-N4 2.30 (2), Si1-N3 1.73(2), Si2-N3 1.70(2), Si3-N4 1.68(2), Si4-N4 1.71(2), N1-C1 1.35(2), N2-C1 1.29(2), N1-Sm-N2 55.4(6), N2-C1-N1 114.9(18) N3-Sm-Si4 136.0(5).

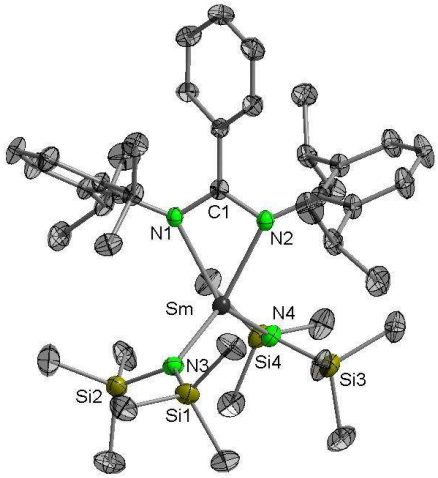

Figure S2. Molecular structure of [Sm$_2$(^{iPr}L$_{DBF}$){N(SiMe$_3$)$_2$}$_4$] (**2**) in the solid state (displacement ellipsoids are scaled to the 30% probability level; omitting carbon bound hydrogen atoms for clarity). Selected bond lengths [Å], angles [°]: Sm-N1 2.421(3), Sm-N2 2.415(3), Sm-N3 2.306(3), Sm-N4 2.297(3), Si1-N3 1.727(3), Si2-N3 1.705(4), Si3-N4 1.715(3), Si4-N4 1.728(4), N1-C1 1.330(5), N2-C1 1.354(5); N1-Sm-N2 55.56(11), N3-Sm-N4 121.49(13), N1-C1-N2 114.2(4).

Table S1. Crystal data and structure refinement for **1** and **2**.

Compound reference	**$[Sm_2(^{iPr}L_{DBF})\{N(SiMe_3)_2\}_4]$**	**$[Sm(^{Dipp}L_{Ph})\{N(SiMe_3)_2\}_2]$**
Chemical formula	$C_{50}H_{106}N_8OSi_8Sm_2$·0.5($C_7H_8$)	$C_{[illegible]}Si_4Sm$·(C_4H_8O)
Formula Mass	1360.84	982.88
Crystal system	orthorhombic	monoclinic
***a*/Å**	10.5585(7)	12.0107(7)
***b*/Å**	20.1286(14)	26.491(2)
***c*/Å**	34.786(3)	17.3028(10)
/°	90	95.898(5)
Unit cell Volume/Å³	7393.0(10)	5476.2(6)
Temperature/K	100	210.0
Space group	*I222*	$P2_1/n$
No. of formula units per unit cell, Z	4	4
Radiation type	MoK	MoK
Absorption coefficient, *m*/mm⁻¹	1.74	1.20
No. of reflections measured	17973	27921
No. of independent reflections	9097	10159
R_{int}	0.0945	0.0431
Final R_1 values (*I*>2(I))	0.0984	0.0386
Final *wR*(F^2) values (*I*>2(I))	0.2236	0.0783
Final R_1 values (all data)	0.1752	0.0710
Final *wR*(F^2) values (all data)	0.2681	0.0836
Goodness of fit on F^2	1.017	0.857

NMR Spectra

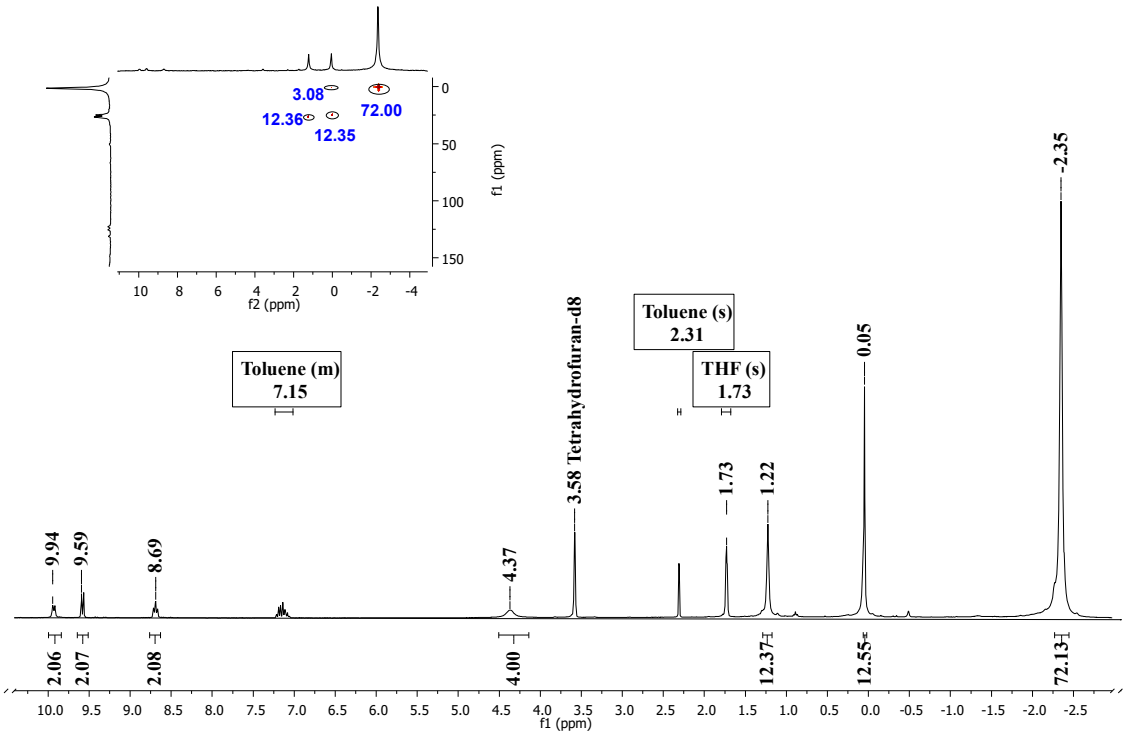

Figure S3. ^{1}H NMR spectrum of [$Sm_2(^{iPr}L_{DBF})\{N(SiMe_3)_2\}_4$] (**1**) in THF-d8.

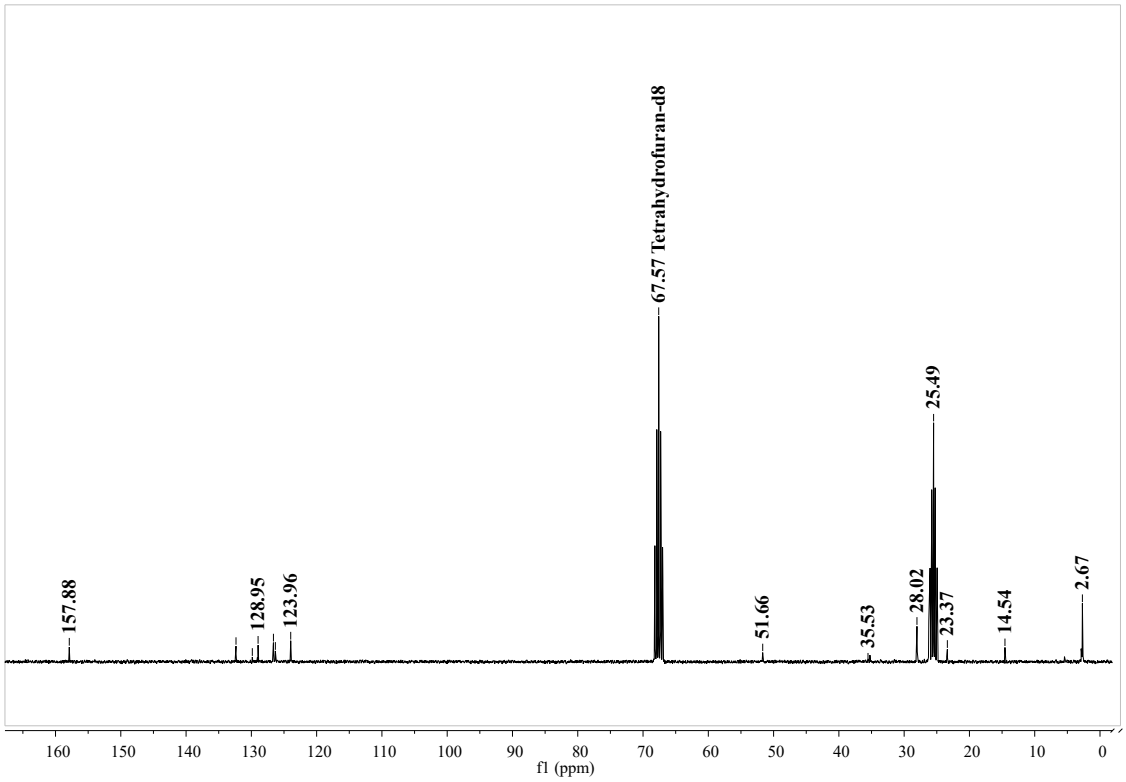

Figure S4. $^{13}C\{^{1}H\}$ NMR spectrum of $[Sm_2(^{iPr}L_{DBF})\{N(SiMe_3)_2\}_4]$ (**1**) in THF-d8.

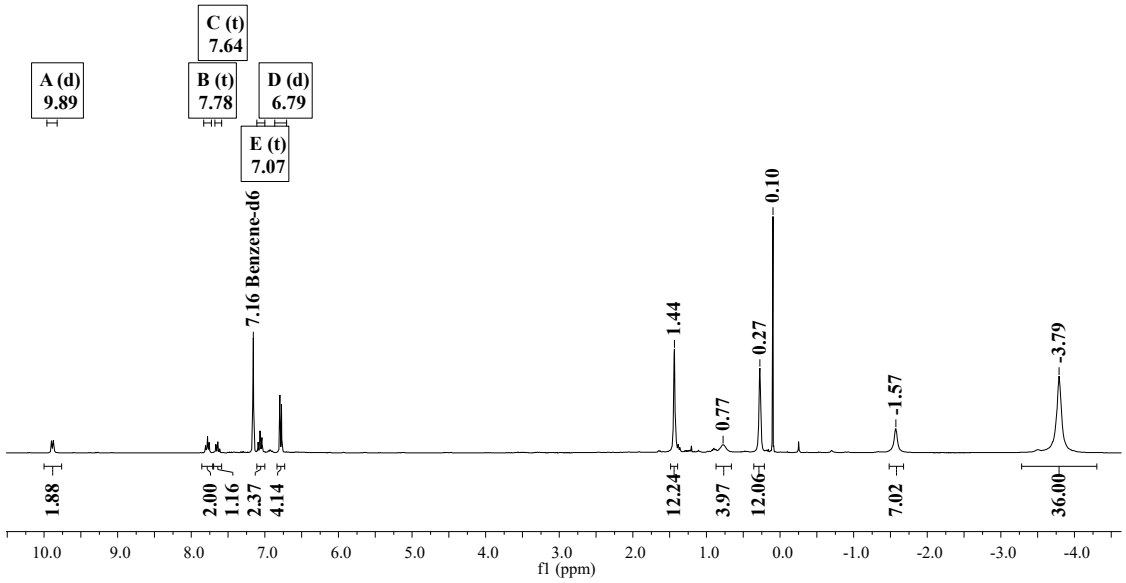

Figure S5. ^{1}H NMR spectrum of [Sm(^{Dipp}L$_{Ph}$){N(SiMe$_3$)$_2$}$_2$] (**2**) in C_6D_6.

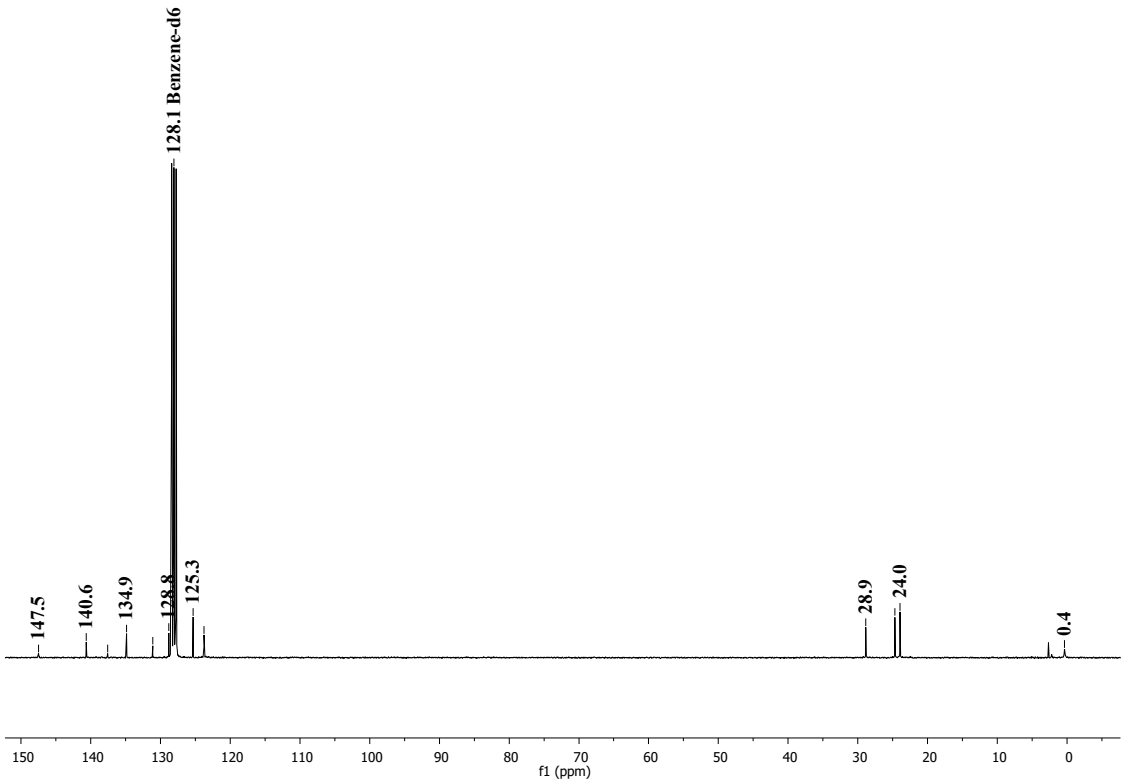

Figure S6. $^{13}C\{^{1}H\}$ NMR spectrum of [Sm($^{Dipp}L_{Ph}$){$N(SiMe_3)_2$}$_2$] (**2**) in C_6D_6.

IR Spectra

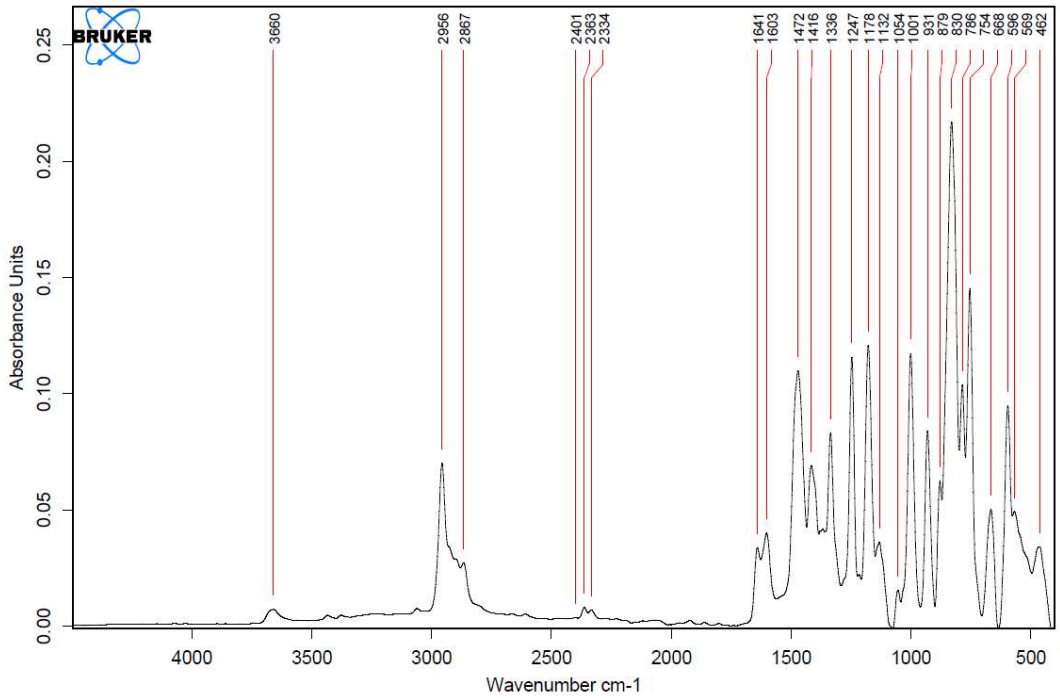

Figure S7. IR (ATR) spectrum of **1**.

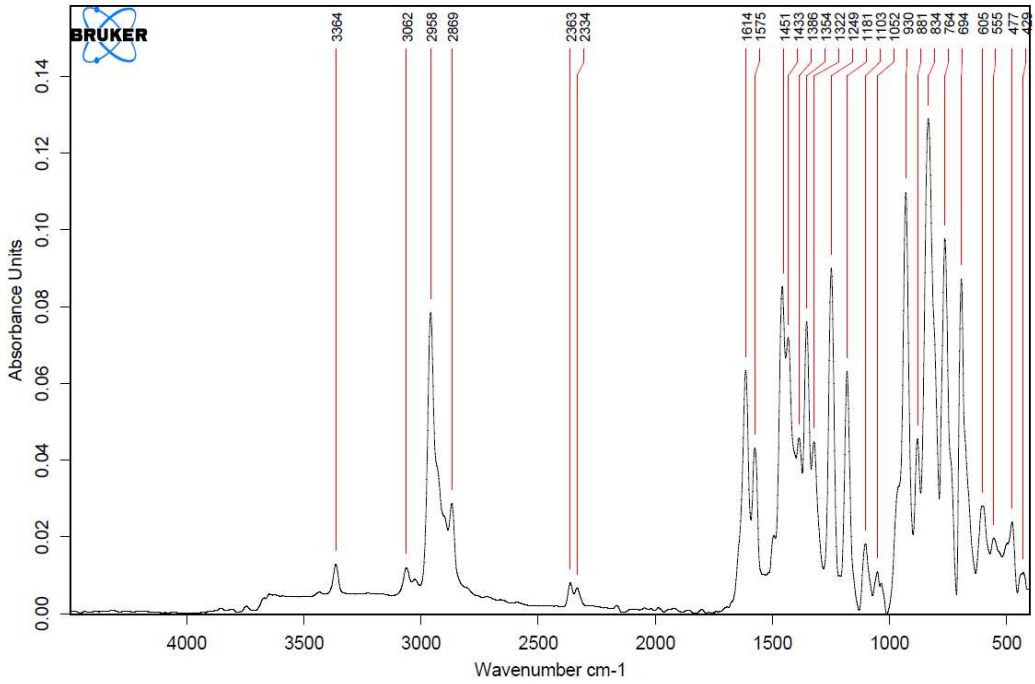

Figure S8. IR (ATR) spectrum of **2**.

Kinetic Measurements

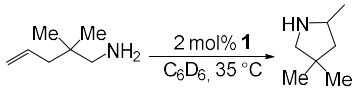

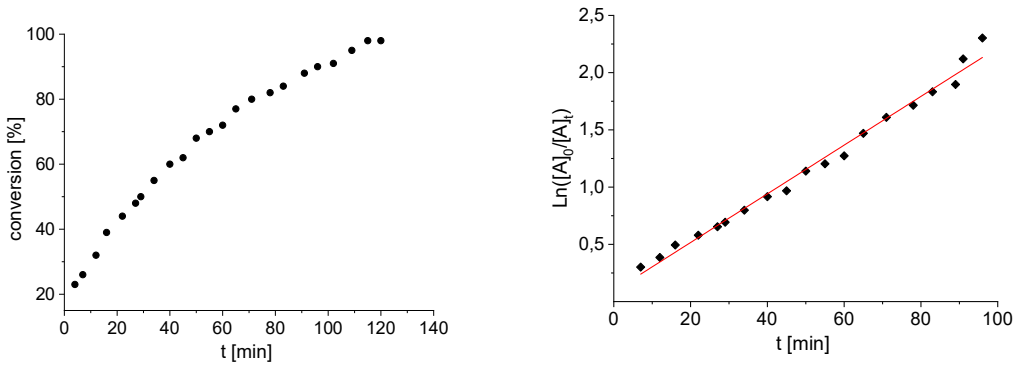

Figure S9. Reaction of **IIIa** with **1** at 35 °C. First order in respect to [substrate] for both reactions. For the determination of the kinetic the final phase (from about 90 % conversion) was cut off; ($y = 0.02127x$; $R^2 = 0.98779$; $k = 0.55 \cdot 10^{-3}\ s^{-1}$); Table 1 Entry 5.

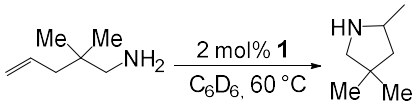

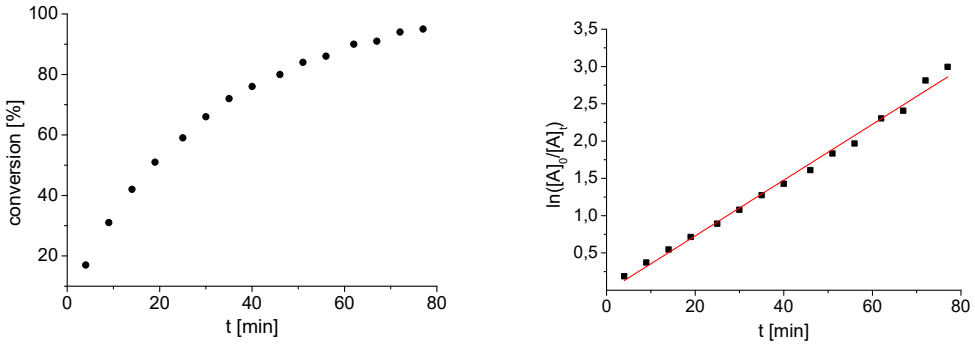

Figure S10. Reaction of **IIIa** with **1** at 60 °C. First order in respect to [substrate] for both reactions. For the determination of the kinetic the final phase (from about 97 % conversion) was cut off; ($y = 0.03740x$; $R^2 = 0.99216$; $k = 0.62 \cdot 10^{-3}\ s^{-1}$).

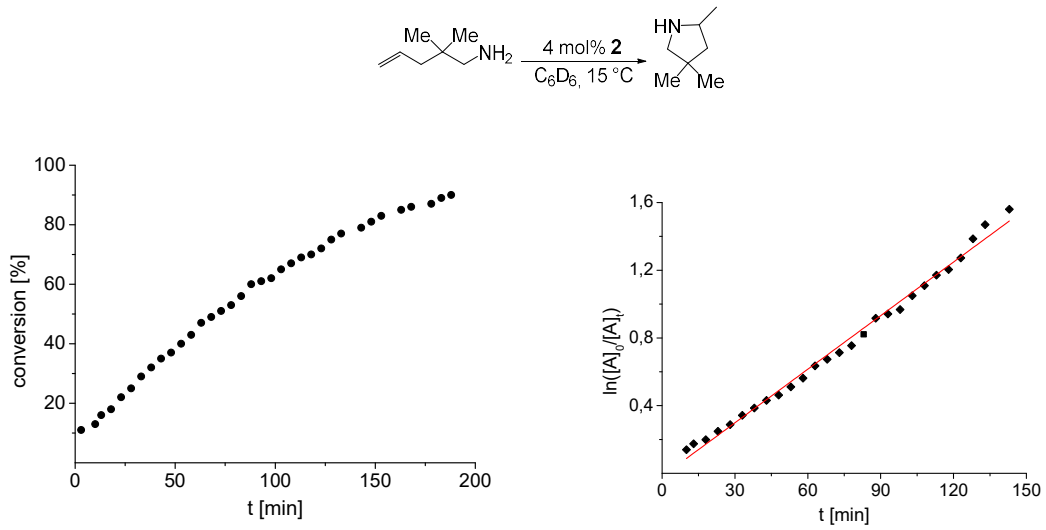

Figure S11. Reaction of **IIIa** with **2** at 15 °C. First order in respect to [substrate] for both reactions. For the determination of the kinetic the final phase (from about 80 % conversion) was cut off; ($y = 0.01055x$; $R^2 = 0.99217$; $k = 0.18 \cdot 10^{-3}\ s^{-1}$).

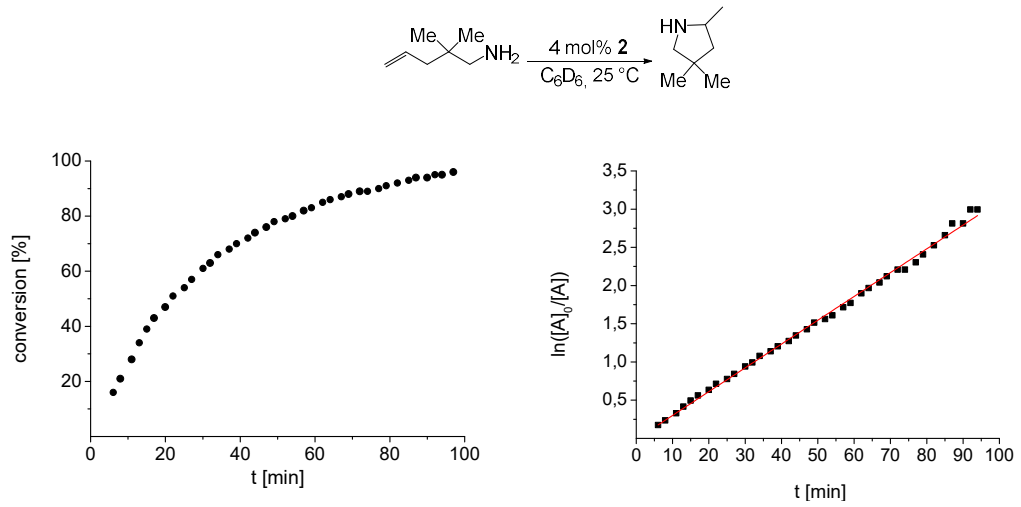

Figure S12. Reaction of **IIIa** with **2** at 25 °C. First order in respect to [substrate] for both reactions. For the determination of the kinetic the final phase (from about 97 % conversion) was cut off; ($y = 0.03114x$; $R^2 = 0.99670$; $k = 0.52 \cdot 10^{-3}\ s^{-1}$.).

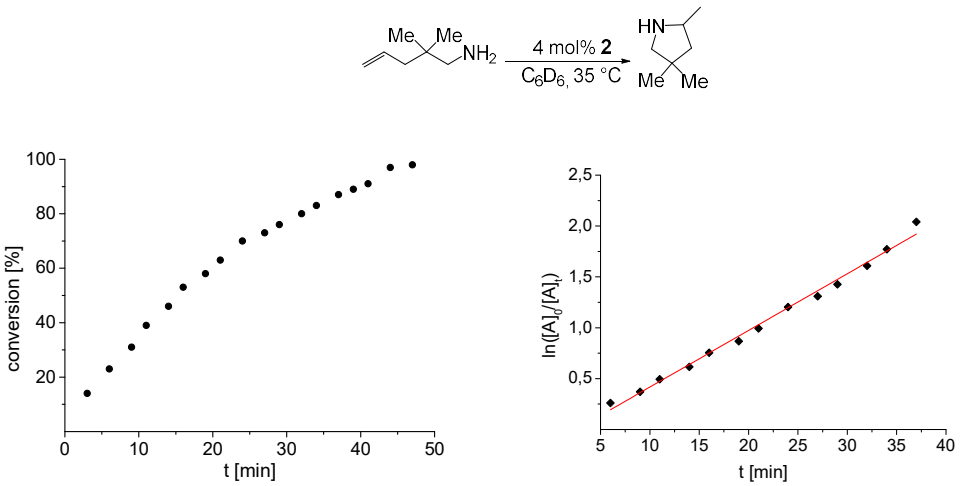

Figure S13. Reaction of **IIIa** with **2** at 35 °C. First order in respect to [substrate] for both reactions. For the determination of the kinetic the final phase (from about 90 % conversion) was cut off; ($y = 0.05570x$; $R^2 = 0.99113$; $k = 0.93 \cdot 10^{-3}$ s^{-1}, Table 1, entry 6.

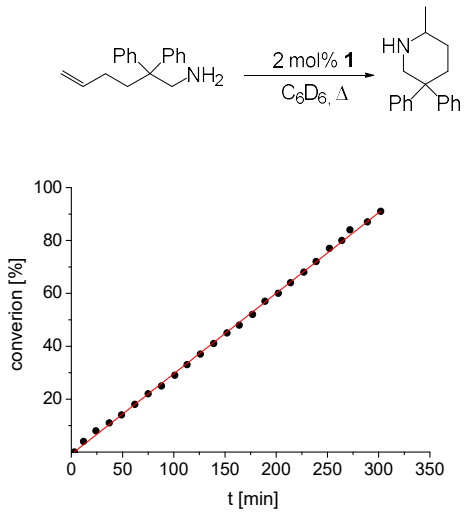

Figure S14. Reaction of **IVa** with **1** at 40 °C. Zero order with respect to [substrate]. For the determination of the kinetic the final phase (from about 90 % conversion) was cut off; $y = 0.30455x$; $R^2 = 0.99915$; $k = 8.11 \cdot 10^{-3}$ (mol/s).

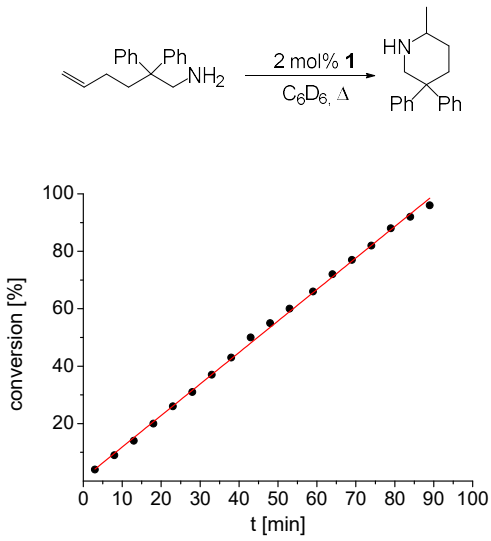

Figure S15. Reaction of **IVa** with **1** at 50 °C. Zero order with respect to [substrate]. For the determination of the kinetic the final phase (from about 90 % conversion) was cut off; y = 1.09700x; R^2 = 0.99870; k = 18.28 · 10^{-3} (mol/s), Table 1, entry 7.

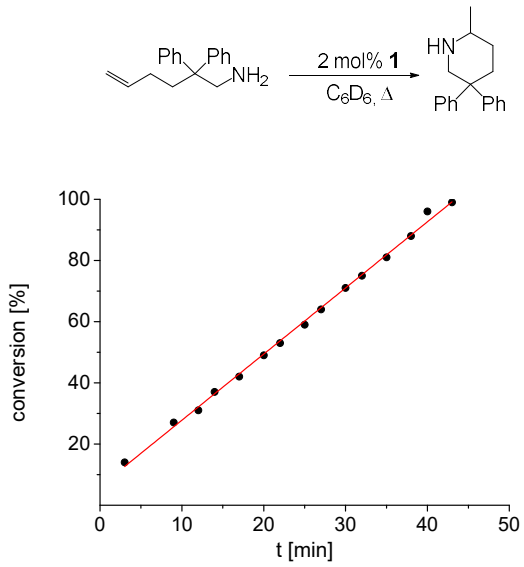

Figure S16. Reaction of **IVa** with **1** at 60 °C. Zero order with respect to [substrate]. For the determination of the kinetic the final phase (from about 90 % conversion) was cut off; y = 2.16194x; R^2 = 0.99764; k = 36.03 · 10^{-3} (mol/s), Table 1, entry 8.

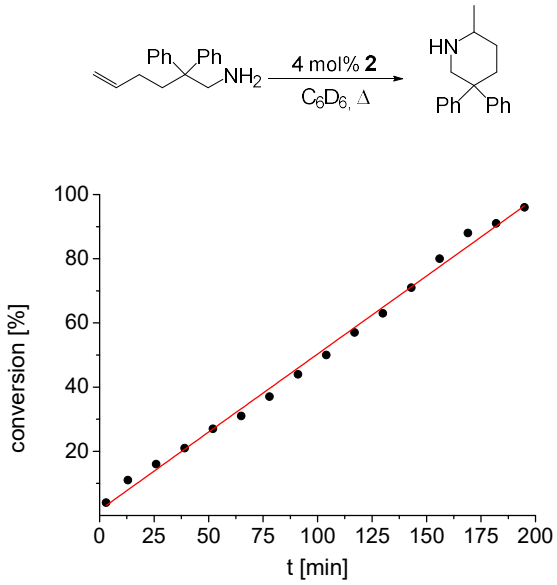

Figure S17. Reaction of **IVa** with **2** at 30 °C. Zero order with respect to [substrate]. For the determination of the kinetic the final phase (from about 90 % conversion) was cut off; y = 0.48634x; R^2 = 0.99495; k = 8.11 · 10^{-3} (mol/s).

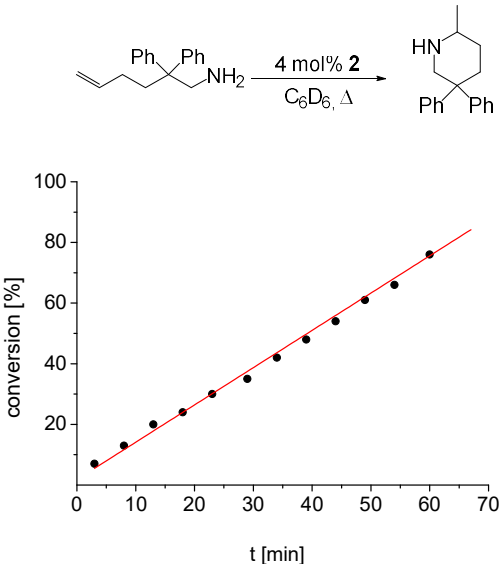

Figure S18. Reaction of **IVa** with **2** at 35 °C. Zero order with respect to [substrate]. For the determination of the kinetic the final phase (from about 90 % conversion) was cut off; y = 1.22936x; R^2 = 0.99078; k = 20.49 · 10^{-3} (mol/s).

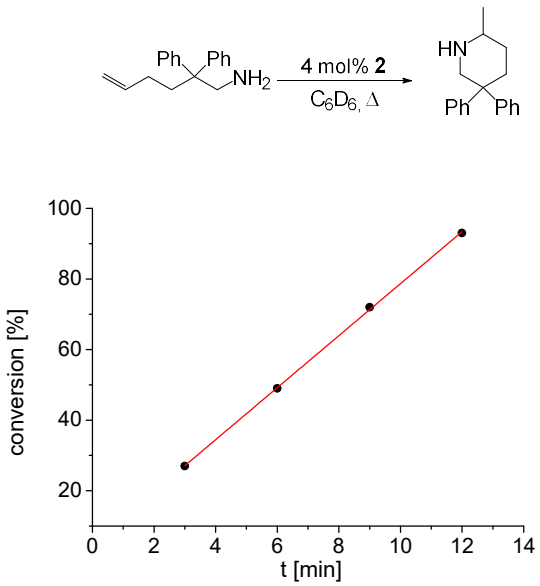

Figure S19. Reaction of **IVa** with **2** at 50 °C. Zero order with respect to [substrate]. For the determination of the kinetic the final phase (from about 90 % conversion) was cut off; y = 7.36667x; R^2 = 0.99957; k = 122.78 · 10^{-3} (mol/s), Table 1, entry 9.

References

1. G. Sheldrick, *Acta Crystallogr. Sect. A*, 2008, **64**, 112-122.
2. G. Sheldrick, *Acta Crystallogr. Sect. C*, 2015, **71**, 3-8.
3. O. V. Dolomanov, L. J. Bourhis, R. J. Gildea, J. A. K. Howard and H. Puschmann, *J. Appl. Crystallogr.*, 2009, **42**, 339-341.